

Markovian city-scale modelling and mitigation of micro-particles from tires

Gunda Obereigner¹, Roman Overko^{2*}, Serife Yilmaz³, Emanuele Crisostomi⁴, Robert Shorten⁵

1 Institute for Design and Control of Mechatronical Systems, Johannes Kepler University, Linz, Austria

2 School of Electrical and Electronic Engineering, University College Dublin, Dublin, County Dublin, Ireland

3 Education Faculty, Department of Mathematics Education, Mehmet Akif Ersoy University, Burdur, Turkey

4 Department of Energy, Systems, Territory and Constructions Engineering, University of Pisa, Pisa, Italy

5 Dyson School of Design Engineering, Imperial College London, South Kensington, London, U.K.

* roman.overko@ucdconnect.ie

Abstract

The recent uptake in popularity in vehicles with zero tailpipe emissions is a welcome development in the fight against traffic induced airborne pollutants. As vehicle fleets become electrified, and tailpipe emissions become less prevalent, non-tailpipe emissions (from tires and brake disks) will become the dominant source of traffic related emissions, and will in all likelihood become a major concern for human health. This trend is likely to be exacerbated by the heavier weight of electric vehicles, their increased power, and their increased torque capabilities, when compared with traditional vehicles. While the problem of emissions from tire wear is well-known, issues around the process of tire abrasion, its impact on the environment, and modelling and mitigation measures, remain relatively unexplored. Work on this topic has proceeded in several discrete directions including: on-vehicle collection methods; vehicle tire-wear abatement algorithms and controlling the ride characteristics of a vehicle, all with a view to abating tire emissions. Additional approaches include access control mechanisms to manage aggregate tire emissions in a geofenced area with other notable work focussing on understanding the particle size distribution of tire generated PM, the degree to which particles become airborne, and the health impacts of tire emissions. While such efforts are already underway, the problem of developing models to predict the aggregate picture of a network of vehicles at the scale of a city, has yet to be considered. Our objective in this paper is to present one such model, built using ideas from Markov chains. Applications of our modelling approach are given toward the end of this note, both to illustrate the utility of the proposed method, and to illustrate its application as part of a method to collect tire dust particles.

1 Introduction

The recent uptake in popularity in vehicles with zero tailpipe emissions is a welcome development in the fight against traffic induced airborne pollutants. The deployment of

such vehicles is consistent with the prevailing contemporary narrative which is heavily focussed on mechanisms to abate mobility related greenhouse gases and tailpipe pollutants; see [1] for a snapshot of some recent work across several disciplines on this topic. However, as vehicle fleets become electrified, non-tailpipe emissions (from tires and brake disks) are likely to become a major concern for human health and this is likely to be exacerbated by the transition to electric vehicles due to their heavier weight and increased torque capabilities [2, 3].

The issue of emissions from tire wear is in itself a very old topic. Somewhat remarkably, issues around the process of tire abrasion, its impact on the environment and human health, and modelling and mitigation measures, remain relatively unexplored and poorly understood. In addition, the general public seems oblivious to the fact that these emissions are significant and almost certainly harmful to human health. The fact that the topic is relatively unexplored and unknown (by the general public) in the context of automotive engineering is very surprising given the rate at which tire mass abrades and contributes to particulate matter (PM) in moving vehicles. PM is a generic term used for a type of pollutants that consists of a complex and varied mix of small particles. There is a growing and rich literature documenting the link between PM and its effects on human health [4–9]. A recent review of the impact of tire and road wear particles can be found in [10]. Roughly speaking, smaller PM particles tend to be directly more harmful to humans compared to larger ones, as they can travel deeper into the respiratory system [6, 11–13] (though larger toxic particles can also cause harm if they enter our food systems). Some of the known health effects related to PM include oxidative stress, inflammation and early atherosclerosis. Other studies have shown that smaller particles may go into the bloodstream and thus translocate to the liver, the kidneys or the brain (see [14] and references within). According to the World

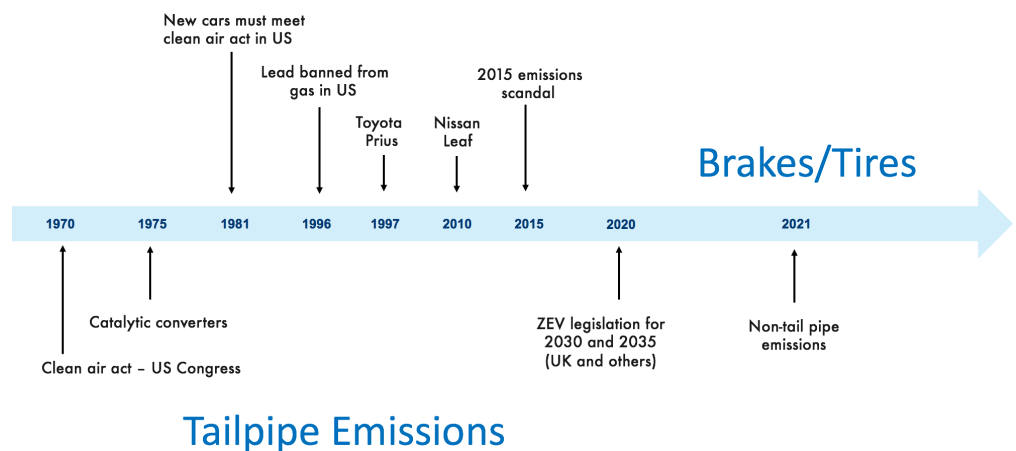


Fig 1. Evolution of recent vehicle emissions narrative, and emerging non-tailpipe emissions concerns.

Health Organisation, for $PM_{2.5}$, the daily maximum deemed safe level on average is $25 \mu g/m^3$, whereas the annual maximum permitted level is on average $10 \mu g/m^3$. For PM_{10} , the maximum permitted levels are on average $50 \mu g/m^3$ and $20 \mu g/m^3$ on a daily and annual basis, respectively. In general, based on these numbers, it is acknowledged that non-exhaust emissions (including brake and tire wear, road surface wear and resuspension of road dust) resulting from road traffic, account for a significant component of traffic related PM emissions [15]. To parse these numbers in the context of a specific city it was recently estimated that approximately 186 kg per day of tire

mass is lost to abrasion in Dublin each day [2].

Recently, the issue of tire generated PM emissions has become a topic of interest for several groups worldwide [16–18]. Roughly speaking, work on this topic has proceeded in several directions with work on the topic focussing on on-vehicle collection methods, on vehicle tire-wear abatement algorithms, or estimating properties of tire debris. For example, several of the authors of [2], *the tire Collective*, have constructed a prototype on-wheel system for collection of tire debris¹. Other authors [19, 20] have explored controlling the ride characteristics of a vehicle with a view to abating tire emissions. A further approach in [2] explores access control mechanisms to manage aggregate tire emissions in a geofenced area. Other notable work on the topic focusses on the particle size distribution of tire generated PM, or to which degree this becomes airborne [8] (while currently available emission factors for tire wear in literature gives estimates of vehicle emissions of between $0.005 - 100g/km$, no reliable method to calculate tire related PM or tire wear, depending, for example, on the vehicle operation, appears to be available [15, 21]). The issue of which particulates become airborne is in fact the subject of some debate in the community. We note strongly that we are **not** concerned with such classifications. While research on emissions has focussed on airborne pollutants, the reality is that both outcomes are problematic for humans. Particles that become airborne have the potential to contribute to poor air quality in cities with all the ensuing health consequences; those that fall to the ground have the potential to enter water systems and contribute to the general problem of environmental microplastic pollution. Thus both manifestations of the tire pollution problem need to be addressed.

Our objective in this paper is to develop city-scale models of tire pollution, for both airborne and non-airborne PM, that can be used to inform policy makers in the fight to mitigate the effect of tire abrasion. We have already mentioned that the issue of tire wear is an old and relatively unexplored topic, in automotive engineering, and is subject to sources of large uncertainty. For example, tire induced PM, depends not only on the chemical composition of tires, but also on traffic densities, speeds, driving styles, and road surfaces. Indeed, the ultimate impact on humans depends on the effect of large aggregations of vehicles, each driven by drivers with differing styles, and with different tires. Given this uncertainty, there is clearly a need for robust and efficient methods that indicate the likely locations where large accumulations of tire mass are likely to be found. We would also like that these models somehow capture the complex relationship between speed limits, traffic signalling, and densities, so that these parameters can be explored from the perspective of tire emissions. To do this we shall build on our previous work on Markovian [22] models of traffic networks. An important point to note in this context is that even though tire emission factors are not well known (perhaps even unknowable), the qualitative aspects of the tire abrasion process is understood (the qualitative effects of speed, acceleration, weight, road surface). This is important from the context of Markovian network emission models which, even though uncertain, do tell us where build ups are likely to occur and the importance of road segments from the context of road debris. We shall show how such models enable a number of important applications in the fight against tire dust; in particular how such models can be used to inform tire dust collection strategies and to inform vulnerable road users such as pedestrians and cyclists.

¹<https://www.youtube.com/watch?v=fo-2b5JzTl8>

2 Markovian models of traffic systems

The use of Markov chains for traffic congestion analysis was first proposed in [22]. Since then the idea has been developed and applied to other traffic related issues in a series of papers [23, 24] and by other authors [25, 26]. For convenience, we now briefly recall some of the background discussion on such models, while a more thorough explanation on such models can be found in the previous references. Traffic flows can be described through a *Markov chain*, which is a stochastic process characterized by the equation

$$p(x_{k+1} = S_{i_{k+1}} | x_k = S_{i_k}, \dots, x_0 = S_{i_0}) = p(x_{k+1} = S_{i_{k+1}} | x_k = S_{i_k}) \quad \forall k \geq 0, \quad (1)$$

where $p(E|F)$ denotes the conditional probability that event E occurs given that event F occurs. Eq (1) states that the probability that the random variable x is in state $S_{i_{k+1}}$ at time step $k + 1$ only depends on the state of x at time step k and not on preceding values. Usually the Markov chain with n states is described by the $n \times n$ *transition probability matrix* \mathbb{P} , whose entry \mathbb{P}_{ij} denotes the probability of passing from state S_i to state S_j in exactly one step. Clearly the matrix \mathbb{P} is a matrix whose rows sum to one (row-stochastic non-negative matrix).

Markov chains are particularly useful for traffic systems due to their close association with graphs (in the context of traffic road networks). Recall that a graph is represented by a set of nodes that are connected through *edges*. Therefore, the graph associated with the matrix \mathbb{P} is a *directed graph*, whose nodes are represented by the states S_i , $i = \{1, \dots, n\}$ and there is a directed edge leading from S_i to S_j if and only if $\mathbb{P}_{ij} \neq 0$. The strong connection between graphs and Markov chains manifests itself in many ways. For example, the notions of chain irreducibility and strongly connected graphs are enunciations of the same concept. More precisely, a graph is *strongly connected* if and only if for each pair of nodes there is a sequence of directed edges leading from the first node to the second one. Thus, \mathbb{P} is *irreducible* if and only if its directed graph is strongly connected. The usefulness of Markov chains for road networks extends well beyond their close relation to graphs. In particular, many easily computable properties of the chain (from the transition matrix) also have strong physical interpretations. For example, for irreducible transition matrices, it is known that the *spectral radius* of \mathbb{P} is 1. This fact is used in applications to detect communities in chains associated with transportation networks. Moreover, the left-hand Perron eigenvector π of the \mathbb{P} matrix, that is $\pi^T \mathbb{P} = \pi^T$ such that $\pi_i > 0$, $\|\pi\|_1 = 1$, yields a closed form expression for the stationary distribution of a random walker over the graph associated with the Markov chain. As such it has a strong connection to likely congestion locations in transportation networks. We shall exploit the Perron eigenvector in the present paper for the purpose of determining likely locations of high tire emissions. Finally, two other quantities that are useful for studying graphs and which can be easily computed are the *Kemeny constant* and the *Mean First Passage Time*. The mean first passage time (MFPT) m_{ij} from the state S_i to the state S_j denotes the expected number of steps to arrive at destination S_j when the origin is S_i , and the expectation is averaged over all possible paths following a random walk from S_i to S_j . If we assume that $m_{ii} = 0$, then the *Kemeny constant* is defined as

$$K = \sum_{j=1}^n m_{ij} \pi_j. \quad (2)$$

Remarkably, the right-hand side is independent of the choice of the origin state S_i [27]. An interpretation of this result is that the expected time to get from an initial state S_i to a destination state S_j (selected randomly according to the stationary distribution π)

does not depend on the starting point S_i [28]. Therefore, the Kemeny constant is an intrinsic measure of a Markov chain. Eq (2) emphasizes the fact that K is only related to the particular matrix \mathbb{P} and it becomes very large if one or more of the other eigenvalues of \mathbb{P} , different from λ_1 , are close to 1.

The use of Markov chains to model road network dynamics has been described in detail in [22] and in many subsequent papers by other authors [25, 26]. The resulting networks are fully characterized by a transition matrix \mathbb{P} , which has the following form:

$$\mathbb{P} = \begin{bmatrix} P_{S_1 \rightarrow S_1} & P_{S_1 \rightarrow S_2} & \cdots & P_{S_1 \rightarrow S_n} \\ P_{S_2 \rightarrow S_1} & P_{S_2 \rightarrow S_2} & \cdots & P_{S_2 \rightarrow S_n} \\ \vdots & \vdots & \ddots & \vdots \\ P_{S_n \rightarrow S_1} & P_{S_n \rightarrow S_2} & \cdots & P_{S_n \rightarrow S_n} \end{bmatrix}. \quad (3)$$

The matrix \mathbb{P} is a square matrix whose size is given by the number of road segments. The off-diagonal elements $P_{S_i \rightarrow S_j}$ are related to the probability that one passes directly from the road segment S_i to the road segment S_j . Importantly, the transition matrix can be very easily computed after gathering the average travel times and junction turning probabilities. In our models the diagonal terms are proportional to travel times. If travel times are computed for all roads, and they are normalized so that the smallest travel time is 1, then the probability value associated to each self-loop is

$$P_{S_i \rightarrow S_i} = \frac{tt_i - 1}{tt_i}, \quad i = \{1, \dots, n\} \quad (4)$$

where tt_i is the average travel time (estimated from collected data) for the i -th road. The off-diagonal elements of the transition matrix \mathbb{P} can be obtained as

$$P_{S_i \rightarrow S_j} = (1 - P_{S_i \rightarrow S_i}) \cdot (tp_{ij}) \quad i \neq j, \quad (5)$$

where tp_{ij} is the turning probability (estimated from collected data) of going from road i to road j [22]. In the next section we shall explain how this basic transition matrix (3) can be modified to convert the model the evolution of tire emissions in an urban landscape.

Comment: The interested reader may ask the advantage of a Markovian model of traffic, as compared with using a traffic simulator, such as SUMO, which we shall extensively use in the remainder of this paper for validation purposes. The principal advantages of a theoretical approach are threefold. First, in terms of utility, once identified, the Markovian model gives access to predictions in a very efficient manner, especially when compared with Monte-Carlo based approaches based on vehicle simulators. Second, following from the previous point, the parameters of mathematical models can be efficiently adjusted to explore traffic management strategies, without the need for ensembles of complex simulations. Finally, by developing a Markovian (transition matrix) approach to traffic modelling, one may avail of a well developed suite of analytics that have been developed to analyse Markovian systems over the past century. This can then be used both to study and analyse the properties of transportation networks, as well as providing a basis for the design of network-level traffic policies. Indeed, this has been explored in a series of papers on traffic modelling since the publication of [22]; see [24] for examples of work in this direction.

3 Extension of Markovian Model to tire Emissions

Our starting point in developing a tire emissions model is the assumption that the Perron eigenvector of a traffic congestion matrix also provides some relevant information about tires' emissions. This is a reasonable assumption because the entries of the Perron eigenvector report the average long-run fraction of time that a vehicle spends on each road. However, there is not a precise relationship between emissions and density information as tires emissions do not only depend on the amount of time that is spent along one road, but also on other quantities, such as average driving style and average speeds. To capture such effects, as a first approximation to develop city-scale models of tire pollution, we shall now describe how the number of tire particles can be estimated depending on the vehicle's speed, and how this information can be embedded in the Markov chain transition matrix.

As we have mentioned, tire emission factors in the literature are characterised by huge uncertainty varying between 0.005 to 100g/km [14]. In any case such a simple characterisation of tire based PM is not suitable to build a Markovian model of tire emissions; to build such a model a tire based PM estimation model depending on a vehicle's operation mode (for example, speed, acceleration, driving style) is required. To this end, we shall use measurements and results from [?] that show a dependency of the number of ultra-fine tire particles PN produced by a vehicle and the vehicle's operation. As particles irrespective of size, tend to be harmful to human health [29] we shall in the sequel focus on the number of particles to evaluate the impact in the city network, and consequently adopt and develop the approach from [?] to estimate the number of particles.

Comment: To further justify our approach it is worth noting the approach adopted here has also been recognised by the latest EU legislative regulations. These place a higher emphasis on the number of particles rather than particle mass or size distribution [30].

The measurements from [?] show a linear dependency of PN and vehicle's speed v , as well as an approximately quadratic dependency of PN and the forces on the wheels F . The combination of both curves leads to the following estimate of PN

$$PN(F, v) = (a_0 + a_1 \cdot F + a_2 \cdot F^2) \cdot (b_0 + b_1 \cdot v). \quad (6)$$

It is not a trivial matter to gather information about values of F and it is therefore more convenient to express F as a function of v (as aggregate estimates of v are simpler to obtain). To do so, we make the simplifying assumption that all roads in the city network are flat (without incline or elevation) and, in addition, for the sake of simplicity, accelerations are neglected.

Comment: The previous assumption introduces some approximations in our estimates (for example, accelerations would cause a higher number of tire particles (6)). However, we make two observations.

- (i) First, it is important to note that if city-wide accelerations can be measured and aggregated, then this approach can be corrected to yield a more realistic and sophisticated model for tire particle estimation.
- (ii) In many of our applications, we are interested in locations of elevated tire dust. While the simplified modelling approach will certainly affect the estimate of absolute amount of PM gathered in a specific location, the relative ranking of

locations (to guide, for example, collection) will be less affected by the modelling assumption.

Thus, in our case, the force can be approximated as a function of velocity as

$$F(v) = m \cdot g \cdot c_r + \frac{\rho A c_d}{2} v^2, \quad (7)$$

where the first term describes the rolling effect of the vehicle, while the second term takes into account the air drag resistance. In Eq (7), m is the mass of the vehicle, g is the gravitational constant, c_r is the rolling resistance, c_d is the drag resistance coefficient, ρ is the density of air, and A is the approximated front area of the vehicle. Numerical values for an average vehicle are given in Table 1. To estimate the number of tire particles per driven km, (6) and (7) are combined as follows:

$$PN(v) = (a_0 + a_1 \cdot \frac{F(v)}{1000} + a_2 \cdot \left(\frac{F(v)}{1000}\right)^2) \cdot (b_0 + b_1 \cdot v) \cdot \frac{1000}{v}. \quad (8)$$

Note that the true process of generating tire particles is also affected by other factors that we are not considering here, such as road surface, type of tire, vehicle's weight [31] etc.

Comment : As a final comment, we further remark that Eq (8) gives the number of particles under rather approximated conditions and may underestimate the actual number of PN , as acceleration and braking events are neglected. However, as the Markovian models reveal densities, we expect these approximations to be reasonably accurate up to a scaling factor.

Table 1. Numerical values for parameters in $PN(v)$ (8).

Parameter	Value	Unit
m	2200	kg
g	9.81	m/s ²
c_r	0.0108	-
ρ	1.2	kg/m ³
A	2.2	m ²
c_d	0.233	-

The estimate of the number of tire particles (8) is now used to convert the unit of time of the original transition matrix into a tire particle, and a step in the Markov chain now corresponds to a unit of tire emission. For this purpose, we change the diagonal entries of the transition matrix \mathbb{P} as follows:

$$P_{S_i \rightarrow S_i} = \frac{PN(v_i) \cdot l_i - 1}{PN(v_i) \cdot l_i}, \quad i = \{1, \dots, n\}, \quad (9)$$

where v_i is the average velocity on the road segment i and l_i is the length of the corresponding road segment. Then, the off-diagonal elements are re-normalized as stated in Eq (5) to keep the transition matrix row-stochastic.

Comment : The effect of the diagonal scaling of Eq (8) is that large values in the diagonal of the original matrix \mathbb{P} of Eq (8) corresponded to long times required to travel along a given road segment, while in the new transition matrix for the tire emissions

model, large values in the diagonal entries of the new transition matrix now correspond to road segments with high tire emissions. More properties of the diagonal scaling can be found in [23]. Table 2 summarizes the interpretation of typical quantities of interest in Markov chains for the original transition matrix of travel times, and the new transition matrix related to tire emissions.

Table 2. Interpretation of some Markov chain quantities of interest in: (a) the case of the Markov chain characterising road congestion; (b) the case of the Markov chain characterising tire emissions.

Quantity / Markov chain	Congestion	Tire emissions
Perron Eigenvector	Vehicular density in the network	Density of tires emissions in the network
Mean First Passage Times	Average travel times for a pair of origin/destination	Average amount of emissions for a pair of origin/destination
Kemeny constant	Average travel time for a random trip (Global indicator of travel efficiency)	Average amount of emissions for a random trip (Global indicator of tires-induced emissions)

4 Applications of tire Emissions Model

While the utility of Markovian traffic models has been documented in several publication, to the best of our knowledge their utility in the context of tire emissions has not yet been investigated. The objective of this section is to present some basic applications of the tire emissions model to illustrate its utility. We begin with some basic applications.

4.1 Application I - Design of Low Emissions Zones

To illustrate potential applications of our approach, we now consider the design of a low emissions zone for a city. To provide some background context and link this to our previous work we now first consider the same urban network that had been investigated in references [22, 23]. This simple network is depicted in Fig 2 and assumes that two clusters of nodes A-B-C and E-F-G are connected through node D. In the diagram nodes correspond to junctions, and links to roads.

It is well known that changing speed limits may be a convenient policy to reduce urban emissions of pollutants. To investigate this idea for tire emissions we now compare what happens if different speed limits are considered in the whole network, and results are illustrated in Fig 3, 4, in terms of the entries of the Perron eigenvector of the stationary distribution of tire emissions. Recall, the entries of the Perron vector are those road segments where tire emissions are most likely to accumulate (both airborne and on the ground).

As it can be seen from Fig 3, 4, measured vehicle obtained from the mobility simulator SUMO² (blue dashed line) are compared with the basic Markovian traffic

²<https://www.eclipse.org/sumo/>

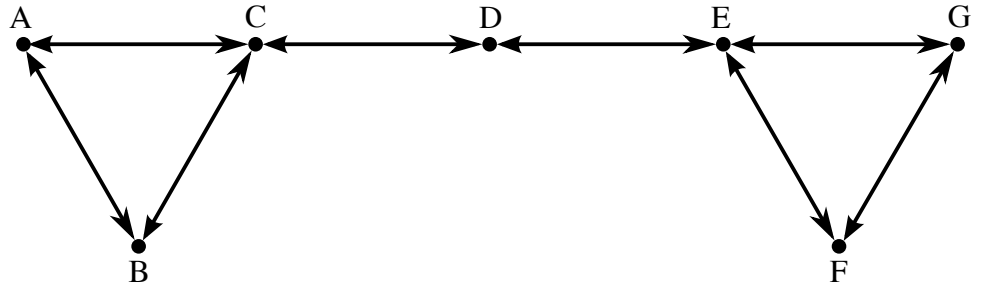


Fig 2. Simple urban network.

model (black solid line), for every considered speed limit. A very close correspondence between the simulator output and the Markov chain can be observed. In the same figure, we also report the distribution of different pollutants as estimated using the Markov chain of emissions [23].

Comment : While the stationary distributions of different pollutants and travel times can be easily estimated with the Markovian approach in a few milliseconds, it is more complicated to retrieve the same information by using the simulator. Indeed, in the latter case an ensemble of simulations has to be carried out for each different value of speed limits, to average the stochastic effects of different routes of different vehicles.

4.1.1 Optimized speed limits

It can be observed in Fig 3 that for low speed limits the density of pollutants is proportional to the density of vehicles (where there are more vehicles, there is more pollution), however, when higher speed limits are considered, the proportionality is lost, and different pollutants exhibit different properties with different speed limits. This last comment is further illustrated in Fig 5 that shows the optimal value of the Kemeny constant as a function of speed limits. Recall that in the context of the tire emissions model, the Kemeny constant K is a measure of the average number of emissions associated with trips in the networks, and thus, it is a single quantity of the Markov chain which can be interpreted as an indication for the pollution in the entire network.

In particular, a lower value the Kemeny constant corresponds to a lower value of average emissions and a better overall network. As we have already observed, this may however be a tricky problem, since the optimal speed limits for tire particles may actually increase emissions from other pollutants. In order to calculate the optimal speed limit for the network, simulations for different maximum speeds, which are 20, 35, 50, 65, 80, 95 km/h, have been conducted using SUMO. After simulating the network for these six different speed limits, and building the resulting Markov chain, six different Kemeny constants can be calculated for each type of pollutant as well as for the travel time. It can be clearly observed that the optimal speed limit varies again for different types of pollutants. While low speed limits seem to be good for reducing CO and tire particles, high speed limits would be better to reduce NOx and of course travel time. Figure 5 depicts the non-obvious result that the “environmentally optimal” speed limit actually depends on the specific pollutant that one is interested in minimizing. In particular, $40km/h$ appears to be the best speed limit if one aims at minimizing CO emissions, $60km/h$ is the best choice for minimizing CO_2 and tire emissions (which is

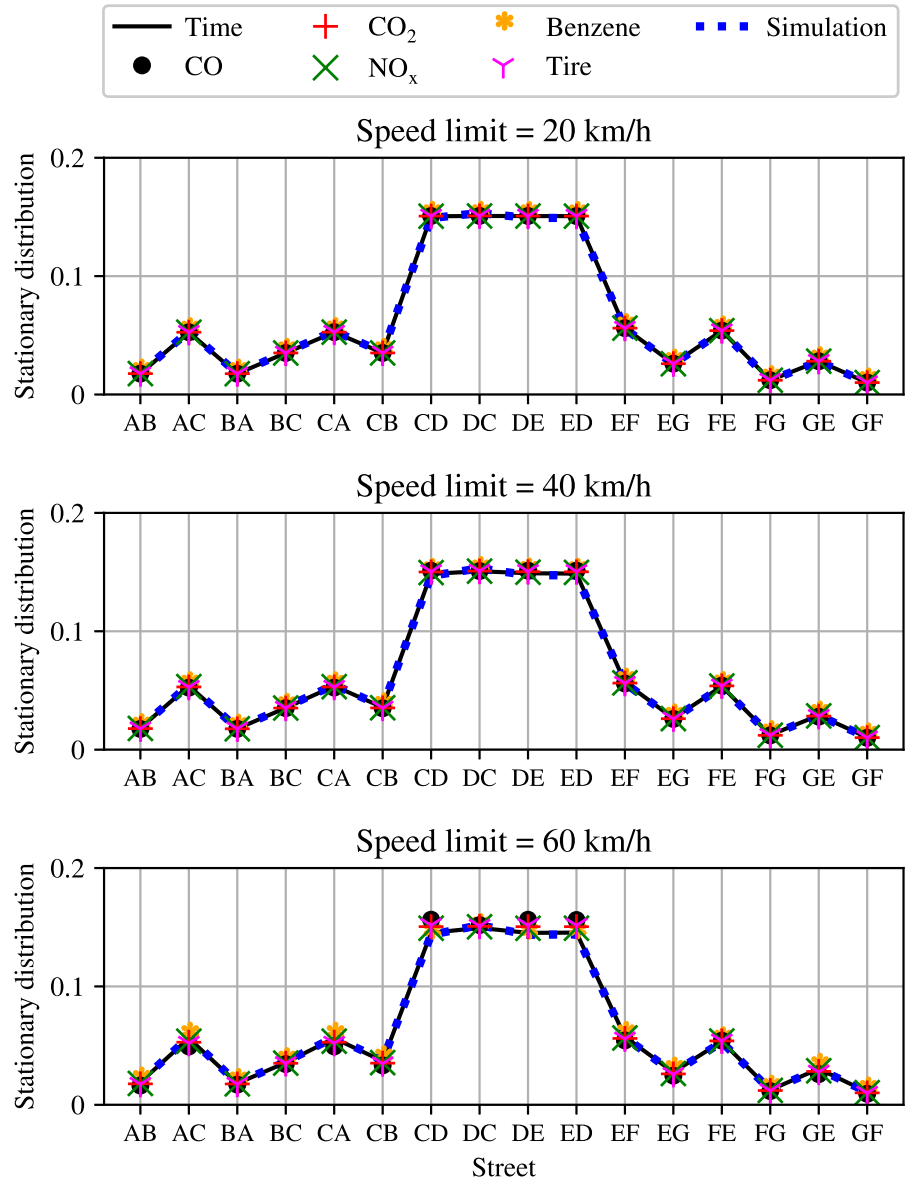


Fig 3. Distribution of emissions for the simple network with different speed limits, namely 20, 40 and 60km/h, in the entire network.

the specific objective of this manuscript), 100km/h is the best choice for minimizing *NOx* and Benzene, while, obviously, the maximum considered speed limit (i.e., 120km/h) is the best option to minimize travel times. Thus, the selections of the “best” speed limits is not trivial, and policy makers should be informed about the optimal speed limits for different pollutants in order to make a decision.

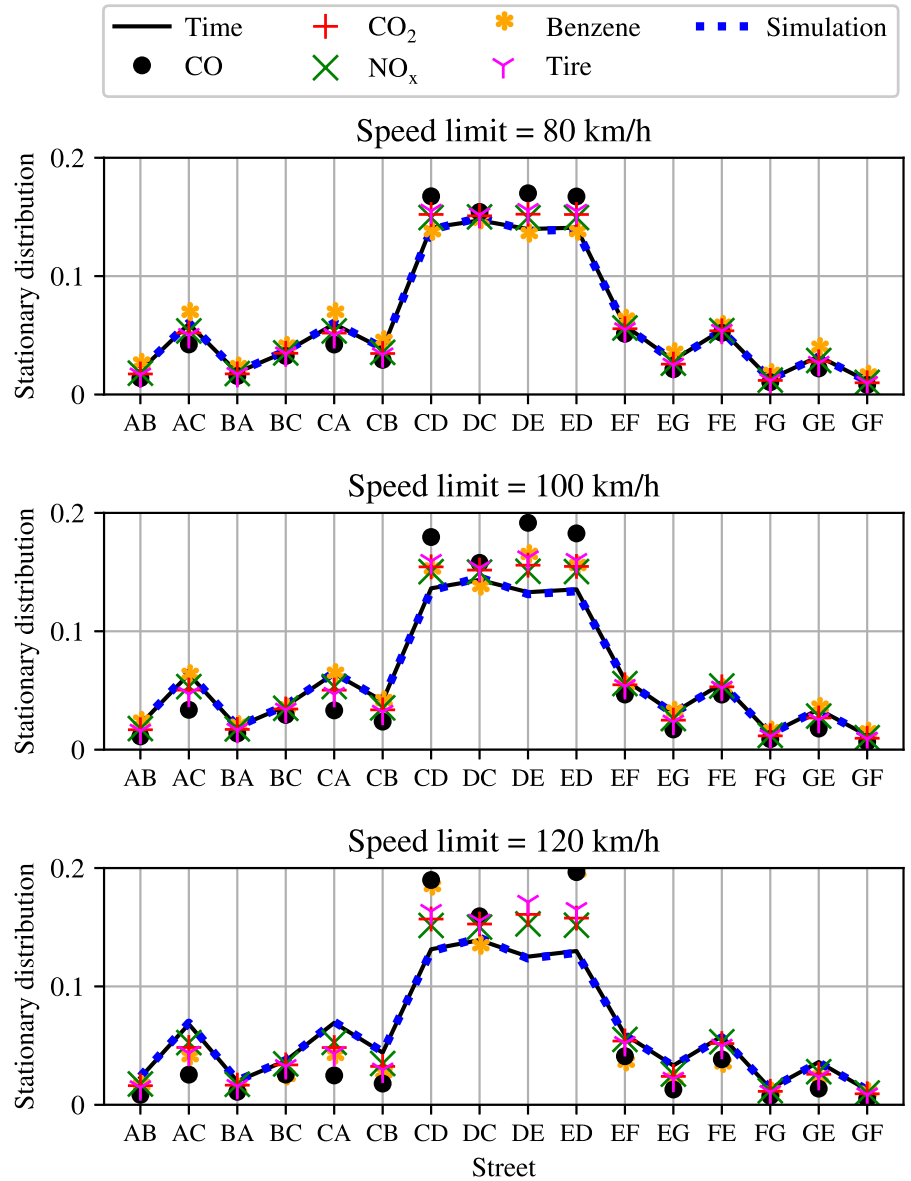


Fig 4. Distribution of emissions for the simple network with different speed limits, namely 80, 100 and 120km/h, in the entire network.

4.1.2 Optimal speed limits in more realistic road networks

To conclude this section we now confirm the above findings on a more realistic road network. To this end, rather than utilising the simple network previously illustrated, we now consider the artificial, but nevertheless realistic, network shown in Fig 6, where we assume that vehicles are allowed to travel in both directions on each road. We simulate the traffic flows utilising the previously mentioned simulator SUMO (Simulation of Urban MObility). SUMO has been developed at the Institute of Transportation

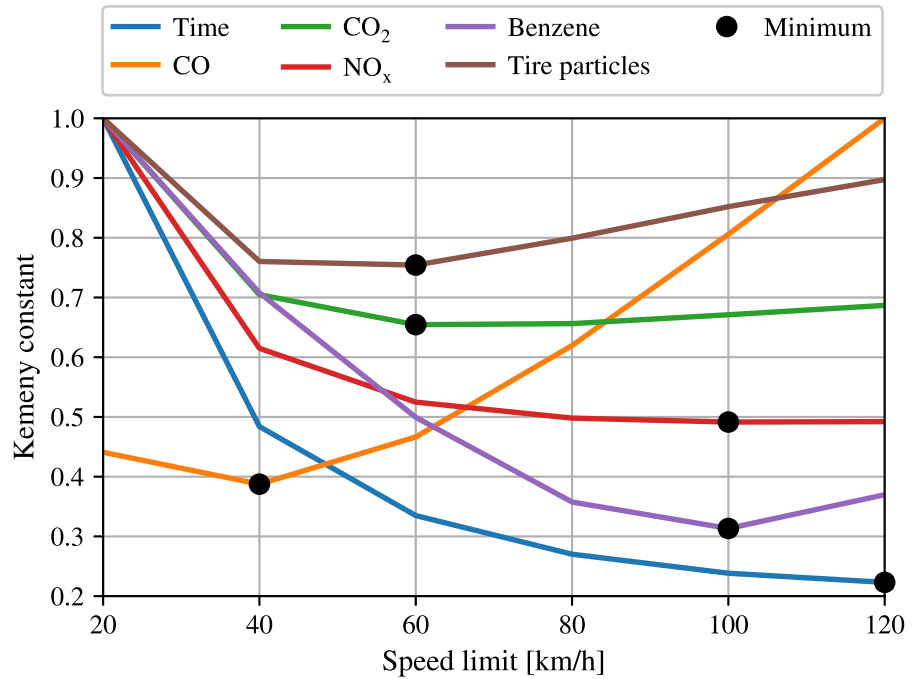


Fig 5. Kemeny constants for the simple network with different speed limits in the entire network.

Systems at the German Aerospace Center and is an open source traffic simulation package that has been frequently used for large traffic networks. Once pre-defined start and destination roads are chosen, SUMO can automatically assign shortest routes to vehicles (e.g., minimum time routes) to the vehicles. After the simulation, statistics such as average travel times, average speeds, junction turning probabilities are available from SUMO for the whole network, and can be used to form the transition matrix \mathbb{P} of travel times. Then, the average speed model can be used to form the transition matrix of tire emissions as explained in Section 3.

As before, in order to calculate the optimal speed limit for the network, simulations for different maximum speeds, which are 20, 35, 50, 65, 80, 95 km/h, have been conducted using SUMO. After simulating the network for these six different speed limits, and building the resulting Markov chain, six different Kemeny constants can be calculated for each type of pollutant as well as for the travel time. Fig 7 shows the Kemeny constants, normalized to fit the same graph. It can be clearly observed that the optimal speed limit varies again for different types of pollutants, confirming the results that had been provided for the simpler network. While low speed limits seem to be good for reducing CO and tire particles, high speed limits would be better to reduce NO_x and of course travel time.

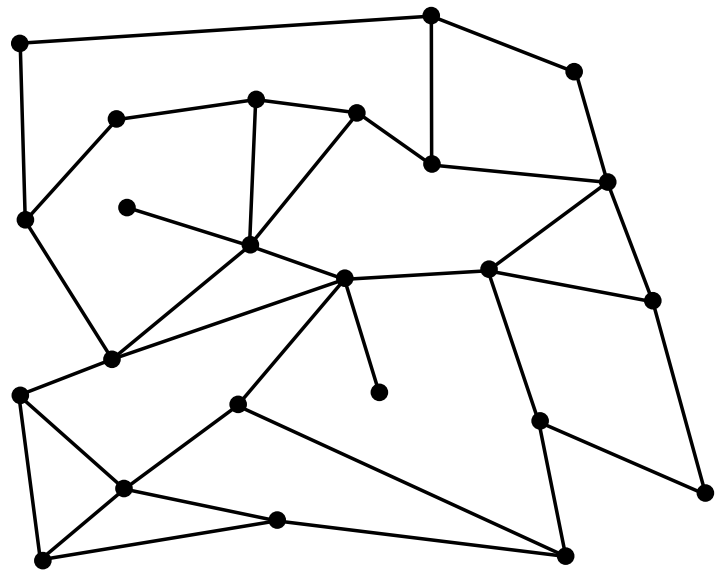


Fig 6. Realistic urban network.

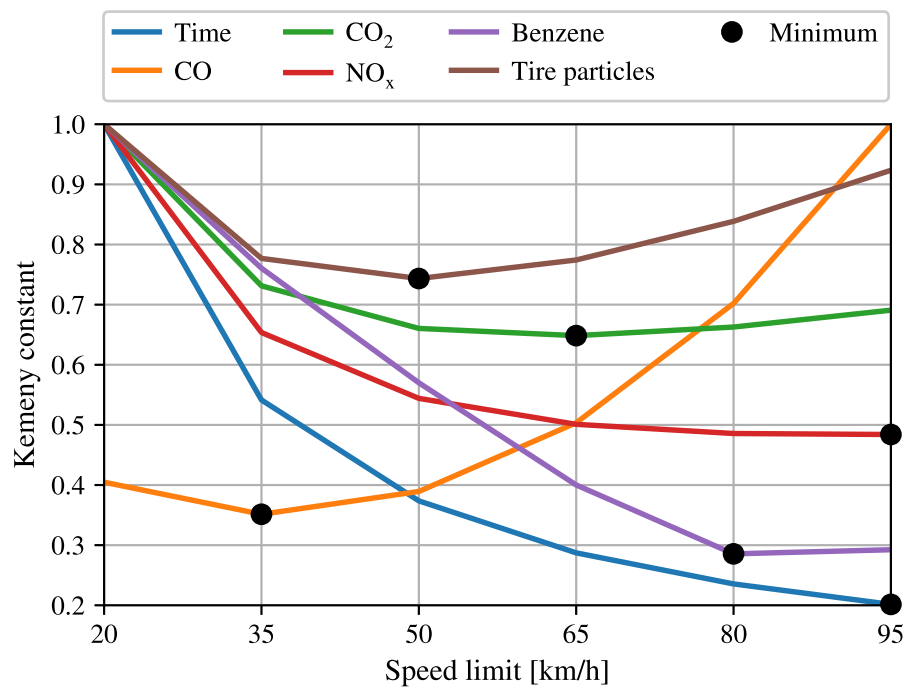


Fig 7. Kemeny constants for the realistic big network with different speed limits in the entire network.

4.2 Application II - Advisory Systems for Protection of Cyclists

One potential application of our Markov chain is related to the tire emissions footprint associated with specific routes. Active travel (cycling, walking) is experiencing a resurgence across the developed world as citizens abandon public transportation in response to health related concerns associated with Covid-19 [32,33]. Pedestrians and cyclists are extremely vulnerable road users and their exposure to traffic emissions regularly far exceeds that of car occupants. Given this context our goal now is to use the Markovian model to find the minimum tire emission route for cyclists in the network in order to reduce the emission exposure and consequently the harmful effect of emissions for their health. Here, we are using the classic Dijkstra algorithm [34] to determine the best route, but different from traditional applications, we do not wish to minimize distance or time, but the exposure to tires emissions. Thus, we associate each road segment with its corresponding entry in the Perron eigenvector (which we remind represents the normalized long run fraction of tire emissions release along each road segment), and we use Dijkstra algorithm to find the best path. In addition to computing the minimum tire emission route, one may also ask whether these best paths are sensitive to changing speed limits; namely, in other words, to know whether changing the speed limits in the network also changes the minimum path. Fig 8 compares the normalized tire emissions along two possible paths, having the same specified origin and destination point, for a cyclists, as a function of speed limits. In particular, path *A* is the shortest path and the minimum emissions path when speed limits are between 20 and 80 km/h whereas path *B* becomes the minimum tire emission path for higher speed limits.

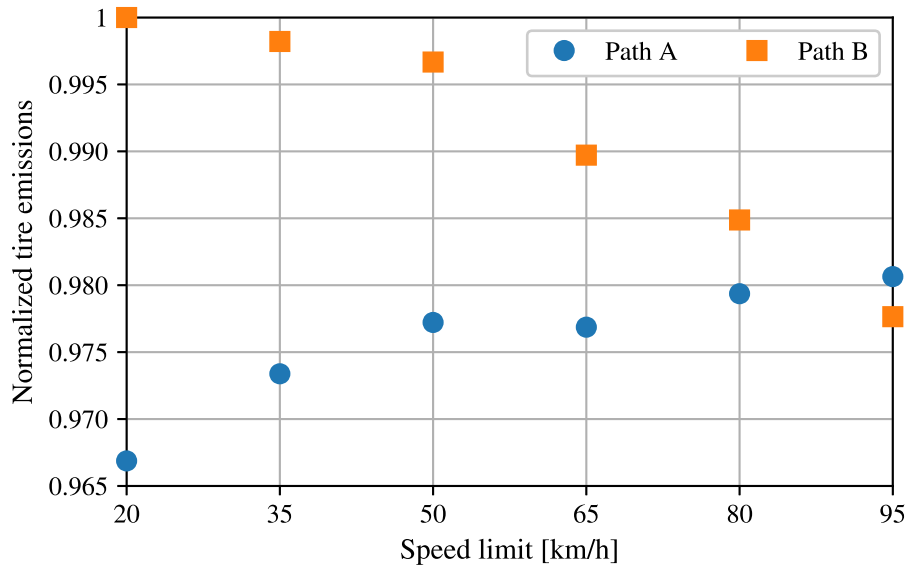


Fig 8. Minimum tire emission route for the realistic big network.

4.3 Application III - Tire-Dust Collection

We now present a somewhat unconventional application of the Markovian approach; namely, using the Markovian approach to inform the collection of tire dust by road sweepers [35]. Street sweeping is an effective practice to reduce the amount of road dust, and there is a recent interest in the literature to evaluate the effectiveness of the process [36] and to improve the efficiency of sweeping machines [37]. Here, we take a different view, and we are rather interested in the path followed by road sweepers. Indeed, we have already mentioned that tire particles are harmful to humans irrespective of whether they become airborne, or become part of ground debris. Ground debris is very harmful to humans due to the various pathways for tire particles to enter the human food system; in particular, through city drainage systems. This latter aspect is an important consideration to motivate the collection of tire particles prior to heavy rainfall events, or other severe weather events. In such circumstances, it is important to collect as much tire debris as quickly as possible, and this is in severe contrast to how road sweeping currently takes place.

Typically, road sweepers follow pre-defined paths, trying to cover most of the city, but without taking into account parts that would maximize the collection of tire particles. In this particular context, our Markovian model has much to offer. Our basic intuition is as follows. Since the Perron eigenvector provides the long-run fraction of pollutants along each road segment, important information can be extracted from the Markov chain to inform collection of tire particles in an optimum manner. However, as we have mentioned - our model is approximate and subject to much uncertainty. Thus, we propose to use our *estimated* chain to seed a learning based algorithm, using Reinforcement Learning (RL), that will learn the routes that are most likely to have large quantities of tire particles, and we now indicate how this can be achieved making use of the Markovian modelling approach.

Recall that reinforcement learning [38] is a machine learning strategy where agents (such as road sweepers) can explore an unknown environment, and learn optimal policies (such as the most likely route to find large quantities of tire particles). Reinforcement learning in conjunction with our Markovian models is appealing for this problem for two reasons.

- (i) Our Markovian model could, in principle, be used as a basis for routing algorithms. However, as mentioned, the model is very uncertain, as it neglects several factors that affect tire particle generation. Thus, using a learning strategy to tune the elements of the transition matrix to provide a basis for routing makes a great deal of sense for such applications.
- (ii) In addition, as we have already mentioned, the Perron eigenvector of the tire emission chain can be used to find the minimum tire emission routes for cyclists and other vulnerable road users. However, the *road sweeping* problem is much more challenging if one wishes to find the *maximum polluted* routes. This problem is an example of longest path problems and these are known to be *NP-hard*. While it is true that longest path problems can sometimes be converted into shortest path problems by negating the edge weights in a graph [39], many shortest path algorithms are able to solve the problem only if the underlying graph does not any cycles. This is not common for road network graphs, thus further motivating our interest in reinforcement learning algorithms.

To orchestrate a setting for reinforcement learning that is *well-posed*, we must first

ensure that negative cycles³ in the graph associated with the network transition matrix are avoided. To avoid such negative cycles in a graph, we simply add travel time/distance constraints to the longest path problem. In addition to making our solution well-posed, such constraints in fact are very sensible for road sweeping applications due to limited battery capacity of sweeping vehicles in the case of electric road sweepers. To this end, we combine the tire emission graph with a distance graph into one directed weighted graph G . Recall that an entry of the Perron eigenvector represents the normalized long run fraction of tire emissions released along the road segment assigned to that entry. The tire emission graph is then obtained by assigning negated entries of the Perron eigenvector to the corresponding edges in the graph. The distance graph is derived from a road network where the edge weight represents the length of road segments included in the corresponding state [40]. This then turns our problem into a type of multi-objective optimisation problem. We use a convex linear combination of the two objectives (travel distance and tire emissions) characterised by a quantity α which is the weight of the distance component of the cost. The corresponding weight function is described in Function 1 which returns the weight of a given edge in graph G . This weight represents the cost of traversing state s from any other preceding state.

Function 1 The Weight Function

Input: $\alpha \in [0, 1]$; $s \in \mathcal{S}$; $l_s, c_s, L_{tot}, C_{tot} \in \mathbb{R}$.

Output: w_s .

- 1: **function** $\mathcal{W}(\alpha, s, l_s, c_s)$
 - 2: $w_s = \alpha * l_s + (1 - \alpha) * \left(-c_s * \frac{L_{tot}}{C_{tot}}\right)$
- return** w_s
-

Notation for the Weight Function: In Function 1 we have: α is the distance weight, a real number that satisfies $0 \leq \alpha \leq 1$; s is a state in the state space \mathcal{S} ; l_s is the length of road links included in state s ⁴; c_s is the amount of tire particles emitted along the road segments included in state s within some given time interval τ ; L_{tot} is the sum of the road lengths for a given road network; C_{tot} is the total amount of tire particles emitted through the entire road network within time interval τ . C_{tot} can be estimated using some historical data, and we simply assume that C_{tot} is known.

To further elaborate on our proposed algorithm, we denote by α_{min} the minimum value of α such that the graph G does not have any negative cycles for weights computed as $\mathcal{W}(\alpha, s, l_s, \bar{c}_s)$, where \bar{c}_s is the estimated amount of tire emissions along the road segments clustered in state s within the time interval τ . The value of \bar{c}_s is the result of multiplication of C_{tot} by the corresponding to state s entry of Perron eigenvector. The value of α_{min} is determined empirically to two decimal digits of precision. Note that even though the weight w_s defined in Function 1 is measured in the units of l_s (i.e., distance), the values of w_s can be negative. This particular design of w_s results in a lower value of α_{min} compared to what one would obtain in the case of normalized unitless weights.

Once a *combined* graph (without any negative cycles) has been constructed, we then use a shortest path algorithm to compute *default solutions*. To deal with values of α such that $\alpha < \alpha_{min}$, approximation techniques are required to find the maximum tire emissions routes subject to the distance constraints. To solve this problem, our

³A negative cycle in a graph is a cycle for which the overall sum of the weights is negative.

⁴The road merging mechanism introduced in [40] is utilised.

preferred approximation tool is reinforcement learning. The *default solutions* from the Markov chain are used as the initial estimate for the reinforcement learning algorithm. Note that even though the number of tire particles is generally larger along longer routes, assigning very long routes to the road sweepers would dramatically increase their travel time and may not even be feasible due to battery constraints.

We employ reinforcement learning to amend the initial estimate whenever the constraint of $\alpha < \alpha_{min}$ is satisfied (note that the case $\alpha = 1$ corresponds to the shortest path routing). The Q-learning algorithm proposed in [41] is utilised here in our work. The initial parameters [38] for the underlying Q-learning algorithm are obtained from the default solutions of the Markovian model. Actions of the agent (i.e. road sweeper) represent road directions, for instance, turn left/right. The goal of the agent is to find a route which maximises the total expected reward [38]. The reward function for this application is outlined in Function 2: it returns a reward at time step t .

Function 2 The Reward Function

Input: $\alpha \in [0, 1]; t, H \in \mathbb{N}; s, s_D \in \mathcal{S}; \beta_1, \beta_2 \in \mathbb{R}^+$.

Output: r_t .

```

1: function  $\mathcal{R}(s)$ 
2:   if  $s \neq s_D$  then                                     ▷ Destination not reached yet
3:     if  $t \neq H$  then                                       ▷ Time horizon not reached yet
4:       Get the length  $l_s$  of road links included in state  $s$ .
5:       Get the estimated amount of pollution  $\bar{c}_s$  in state  $s$ .
6:       Measure the actual amount of pollution  $c_s$  emitted in state  $s$ .
7:       // Compute weights for state  $s$ 
8:        $\bar{w}_s = \mathcal{W}(\alpha, s, l_s, \bar{c}_s)$ ,  $w_s = \mathcal{W}(\alpha, s, l_s, c_s)$            ▷ Calls to Function 1
9:        $r_t = 1 - \frac{\bar{w}_s}{w_s}$ 
10:    else                                                       ▷ Time horizon reached
11:       $r_t = -\beta_2$                                              ▷ Penalty
12:    else                                                       ▷ Destination reached
13:       $r_t = \beta_1$ 
14:    return  $r_t$ 

```

Notation for the Reward Function: The notation for Function 2 is as follows. H is the time horizon, i.e. the number of allowed transitions per episode (day). State s_D is the destination state. The parameter β_1 represents a reward that an agent would receive if it reached the destination state. Finally, β_2 is a reward given to the agent if it did not reach the destination within H times steps.

A realistic road network, based on an existing area in Barcelona, Spain, used in all our experiments is depicted in Fig 9. To illustrate our algorithm we describe several illustrative experiments, designed using the SUMO traffic simulator and randomly generated traffic conditions. In all our experiments, a single Q-learning agent, i.e. road sweeper, starting from the same origin O (see Fig 9) each episode (day) is used. The agent has a fixed destination D to which it is asked to find the optimal route which (i) should be most polluted, and (ii) satisfies the distance constraint given by the parameter α . A road sweeper is released every time a new episode starts, i.e., once per day. Regarding the design parameters in the reward function, the values of β_1 and β_2 were tuned to be 3 and 8, respectively. The values of α_{min} were empirically determined for each specific experiment.

4.3.1 Experiment 1: Tire dust collection under high traffic densities

In this experiment, we firstly consider a scenario in which traffic density is high. To achieve such a condition, we release a new vehicle every simulation step. High traffic density conditions naturally result in a larger amount of tire dust on the streets. In these settings, the estimated value of α_{min} is 0.78.

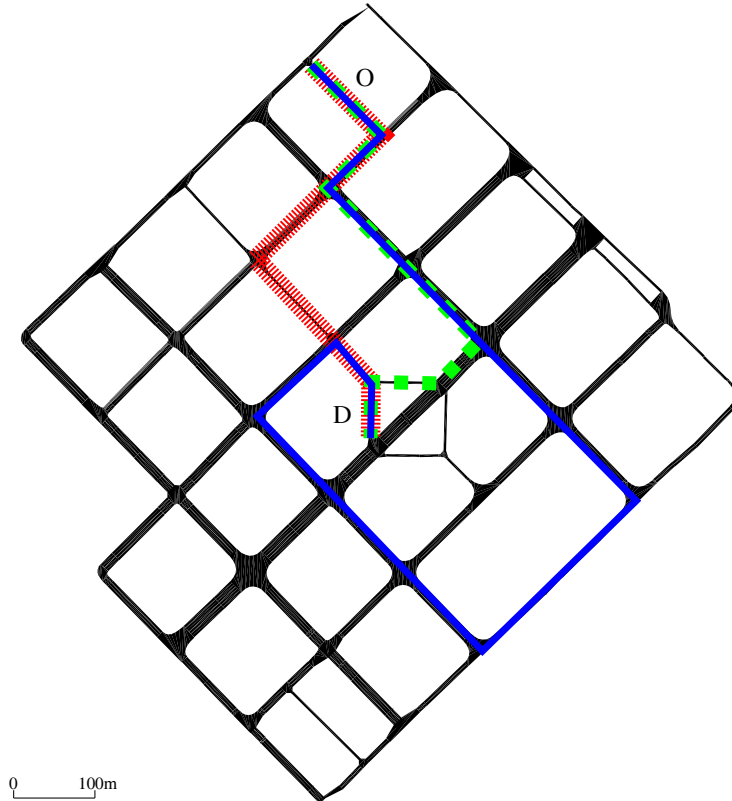


Fig 9. Realistic road network used in the experiments: an area in Barcelona, Spain. The road networks includes 153 road links which were clustered in 62 states. Fixed origin O and destination D are used in the experiments. Note: the route marked with red is the shortest path route from O to D; the green route is the default solution; and the blue one represents a solution provided by the Q-learning algorithm under high traffic density.

Fig 9 shows the shortest path in red, the initial solution in dashed green, and the optimal solution in solid blue, obtained using the proposed Q-learning algorithm for high traffic densities. Fig 10 compares the properties of such three routes with $\alpha = 0.5$ used for the Q-learning solution. The brown dot-dashed line corresponds to the shortest path route, which was calculated using Dijkstra shortest path algorithm on the graph with weights computed using Function 1 for $\alpha = 1$. The blue dashed line corresponds to the route obtained from the initial estimate, i.e., the default solution. Such a route was also calculated using Dijkstra shortest path algorithm on a graph with weights computed using the same weight function for $\alpha = \alpha_{min} = 0.78$. As it can be seen in Fig 10 (black solid line), the road sweeper uses the initial solution at the beginning of the learning process. The agent, however, can explore the environment by taking random actions and eventually improves the chosen sweeping path. As it can be

observed, the agent is able to find much longer routes than the shortest path and default routes in a rapid fashion, and such routes are also more polluted with tire particles. Even though routes with higher tire emissions have been explored by the agent, it will not prefer them due to the distance constraint, and this Q-learning routing system eventually converges to the solution which is optimal for the selected value of α .

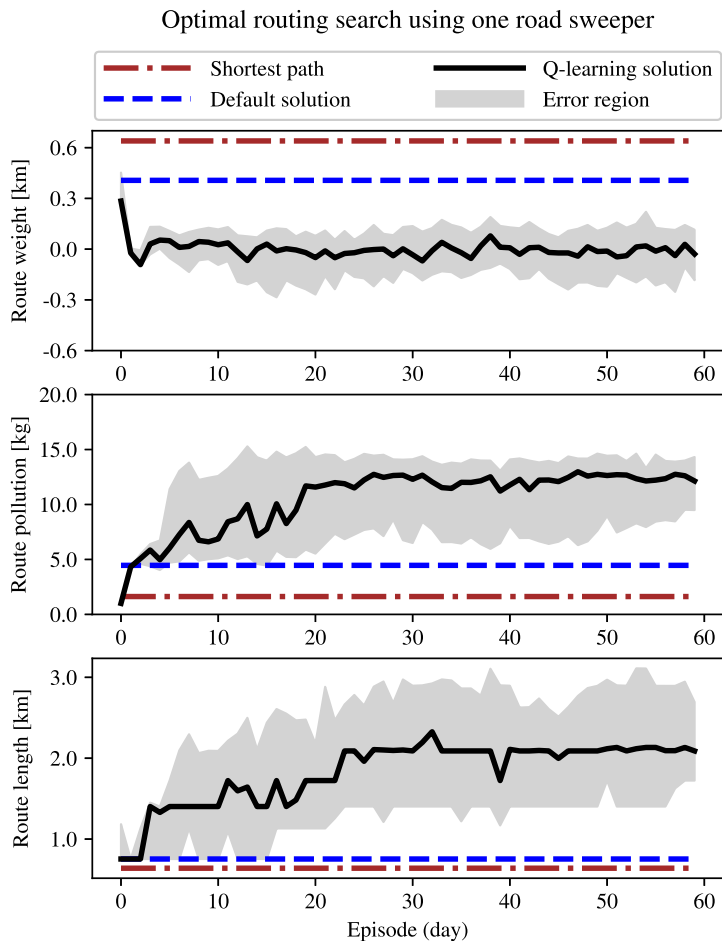


Fig 10. Comparison of the shortest path routing, the initial solution ($\alpha_{min} = 0.78$) and Q-learning solution for $\alpha = 0.5$ under high density traffic conditions. The black curve corresponds to the median value of 100 different realizations of the experiment. The error region indicates the 30th and 70th percentiles.

4.3.2 Experiment 2: Tire dust collection under low traffic densities

To simulate traffic conditions with a lower density, a new vehicle is now released every second simulation step. In this case, the obtained value of α_{min} is 0.79. Fig 11 depicts the shortest path, default solution, and performance of Q-learning for $\alpha = 0.4$. For low densities, it is reasonable to reduce the value of α in order to give more priority to pollution over distance. Otherwise, the Q-learning routing system would be useless as it may converge to the default solution. Note that the amount of collected pollution by

the road sweeper in this case is indeed lower than that in the case of high density traffic (see the middle subplots in Fig 10 and Fig 11).

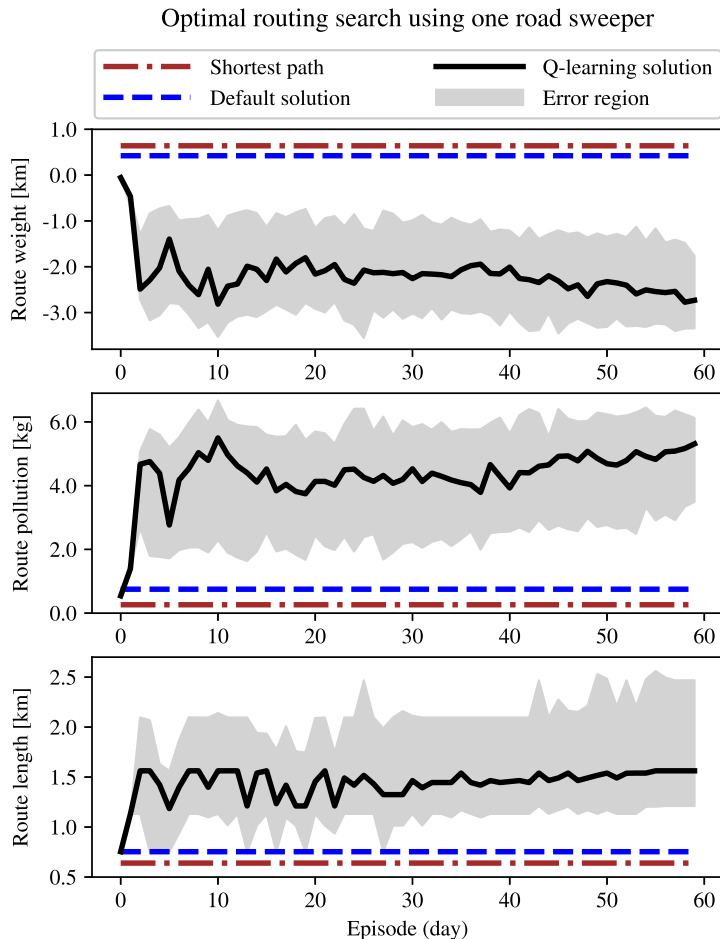


Fig 11. Comparison of the shortest path routing, the default solution ($\alpha_{min} = 0.79$) and Q-learning solution for $\alpha = 0.4$ under low density traffic conditions. The black solid curve is the median value of 100 different realizations of the experiment. The error region indicates the 30th and 70th percentiles.

From Experiment 1 and Experiment 2, we can draw the conclusion that the system is indeed able to find the optimal solution (the most polluted route with tire particles, without breaking travel distance/time constraints) in both high and low density traffic conditions. Thus, the RL strategy is an attractive alternative to those tools that can be fragile, especially when dealing with longest path problems and large-scale scenarios.

Conclusion

The problem of tire dust collection is likely to become one of the most pressing issues in automotive research and in wider society. While the problem of micro-plastic pollution is already becoming an issue of concern, the problem of tire induced pollution has,

remarkably, yet to manifest itself in the consciousness of the public-at-large, possibly due to the sheer weight of the zero-tailpipe narrative that prevails currently in public discourse. Our objective in this paper is thus twofold. First, we wish to make researchers across a wide spectrum of disciplines, aware of this problem, in all its guises. Second, we wish to suggest mitigation measures that can be used to combat this problem. While previous studies have focussed on *on-vehicle* mitigation measures, and network level *access control mechanisms*, our approach here is somewhat different. Our approach is to develop modelling strategies that can be deployed *a-posteri*. Specifically, we wish to predict, using a combination of measurements, and analytics, the likely areas where tire-dust will aggregate, with a view to using this information to inform collection strategies. In this paper we have introduced one such model of tire dust distribution in cities. A number of application use-cases are suggested that use the main features of this model. Future work will explore refinements of this initial model and its experimental validation.

References

1. Crisostomi, E., Shorten, R., Stüdl, S., Wirth, F., “Electric and Plug-in Hybrid Vehicle Networks”, CRC-Press, 2017.
2. Katsikouli P., Ferraro P., Richardson H., Cheng H., Anderson S., Mallya D., Timoney D., Masen M., and Shorten R., “Distributed Ledger Enabled Control of tire Induced Particulate Matter in Smart Cities”, *Frontiers in Sustainable Cities*, Vol 2, pp. 48-58, 2020.
3. Prenner, S., Allesch, A., Staudner, M., Rexeis, M., Schwingshackl, M., Huber-Humer, M., Part, F., “Static modelling of the material flows of micro- and nanoplastic particles caused by the use of vehicle tyres”, *Environmental Pollution*, Volume 290, 2021.
4. Valavanidis, A., Fiotakis, K. and Vlachogianni, T., “Airborne particulate matter and human health: toxicological assessment and importance of size and composition of particles for oxidative damage and carcinogenic mechanisms”, *Journal of Environmental Science and Health, Part C*, Vol. 26, No. 4, pp. 339-362, 2008.
5. Gehring, U., Beelen, R., Eeftens, M., Hoek, G., de Hoogh, K., de Jongste, J., Johan, C., Keuken, M., Koppelman, G., Meliefste, K., Oldenwening, M., Postma, D., van Rossem, L., Wang, M., Smit, H., Brunekreef, B., “Particulate matter composition and respiratory health: the PIAMA Birth Cohort Study”, *Epidemiology* Vol. 26, No. 3, pp. 300-309, 2015.
6. European Environmental Agency, “Air Quality in Europe 2014 report”, Available at:
<http://www.eea.europa.eu/publications/air-quality-in-europe-2014>, 2014.
7. Laden, F., Schwartz, J., Speizer, F. E. and Dockery, D. W., “Reduction in fine particulate air pollution and mortality: extended follow-up of the Harvard Six Cities study”, *American journal of respiratory and critical care medicine*, Vol. 173, No. 6, pp. 667-672, 2006.
8. Amato, F., Cassee, F.R., van der Gon, H.A.D., Gehrig, R., Gustafsson, M., Hafner, W., Harrison, R.M., Jozwicka, M., Kelly, F.J., Moreno, T. and Prevot,

- A.S., "Urban air quality: the challenge of traffic non-exhaust emissions", Journal of hazardous materials Vol. 275, pp. 31-36, 2014.
9. de Miranda, R. M., de Fatima Andrade, M., Fornaro, A., Astolfo, R., de Andre, P. A. and Saldiva, P., "Urban air pollution: a representative survey of $PM_{2.5}$ mass concentrations in six Brazilian cities", Air Quality, Atmosphere and Health, Vol. 5, No. 1, pp. 63-77, 2012.
 10. Baensch-Baltruschat, B., Kocher, B., Stock, F., and Reifferscheid, G., "Tire and road wear particles (TRWP) - A review of generation, properties, emissions, human health risk, ecotoxicity, and fate in the environment", Science of The Total Environment, Vol. 733, 2020.
 11. Chen, H., Kwong, J.C., Copes, R., Tu, K., Villeneuve, P.J., Van Donkelaar, A., Hystad, P., Martin, R.V., Murray, B.J., Jessiman, B. and Wilton, A.S. , "Living near major roads and the incidence of dementia, Parkinson's disease, and multiple sclerosis: a population-based cohort study", The Lancet, pp.718-726, 2017.
 12. Hatzopoulou, M. and Miller, E. J., "Linking an activity-based travel demand model with traffic emission and dispersion models: Transports contribution to air pollution in Toronto", Transportation Research Part D: Transport and Environment, Vol. 15, No. 6, pp. 315-325, 2010.
 13. WHO (World Health Organization), "Health effects of particulate matter. Policy implications for countries in eastern Europe, Caucasus and central Asia", 2013.
 14. Grigoratos, T. and Martini, G., "Non-exhaust traffic related emissions. Brake and tire wear PM", Report EUR, No. 26648, 2014.
 15. Timmers, V. R. and Achten, P. A., "Non-exhaust PM emissions from electric vehicles", Atmospheric Environment, Vol. 134 , pp. 10-17, 2016.
 16. Kole, P. J., Lohr, A. J., Van Belleghem, F. and Ragas, A., "Wear and tear of tires: a stealthy source of microplastics in the environment", International journal of environmental research and public health, Vol. 14, No. 10, 2017.
 17. Grigoratos, T., Gustafsson, M., Eriksson, O. and Martini, G., "Experimental investigation of tread wear and particle emission from tires with different treadwear marking", Atmospheric Environment, Vol. 182, pp. 200-212, 2018.
 18. Keuken, M., Hugo D., and Karin V., "Non-exhaust emissions of PM and the efficiency of emission reduction by road sweeping and washing in the Netherlands", Science of the total environment Vol. 408, No. 20, pp. 4591-4599, 2010.
 19. Obereigner, G., Shorten, R., Meier, F., Jones, S. et al., "Active Limitation of Tire Wear and Emissions for Electrified Vehicles," SAE Technical Paper 2021-01-0328, 2021.
 20. Obereigner, G., Shorten, R., del Rey, L., "Low tire Particle Control", Proceedings of IEEE International Conference on System Theory, Control, and Computing, 2020.
 21. Fauser, P., Tjell, J. C. and Bjerg, P. L., "Particulate air pollution, with emphasis on traffic generated aerosols", 1999.

22. Crisostomi E, Kirkland S, Shorten R. (2011). "A Google-like model of road network dynamics and its application to regulation and control". *International Journal of Control*. Vol 81, No. 3, pp. 633–651., 2011.
23. Crisostomi, E., Kirkland, S., Schlote, A., and Shorten, R., "Markov chain based emissions models: a precursor for green control", *Green IT: Technologies and Applications*, pp. 381–400., Springer, 2011.
24. Faizrahnemoon, M., Schlote, A., Maggi, L., Crisostomi, E., Shorten, R., "A big-data model for multi-modal public transportation with application to macroscopic control and optimisation", *International Journal of Control*, Vol. 88, No. 11, pp. 2354–2368, 2015.
25. Wang, T., Cao, J., Hussain, A., "Adaptive Traffic Signal Control for large-scale scenario with Cooperative Group-based Multi-agent reinforcement learning", *Transportation Research Part C: Emerging Technologies*, Vol. 125, pp. 103046, 2021.
26. Besenczi, R., Bátfai, N., Jeszenszky, P., Major, R., Monori, F., Ispány, M., "Large-scale simulation of traffic flow using Markov model", *PLOS ONE*, 1-31, 2021.
27. Kemeny J.G., Snell J.L., "Finite Markov Chains", Van Nostrand, 1960.
28. , Doyle, P., "The Kemeny constant of a Markov chain, ArXiv preprint:0909.2636, 2009.
29. Schraufnagel, D., "The health effects of ultra-fine particles", *Experimental and Molecular Medicine*, Vol. 52, pp. 311-317, 2020.
30. Regulation (EC) No 715/2007 of the European Parliament and of the Council of 20 June 2007 on type approval of motor vehicles with respect to emissions from light passenger and commercial vehicles (Euro 5 and Euro 6) and on access to vehicle repair and maintenance information, OJ L 171, 29.6.2007.
31. Jekel, M., "Scientific report on tire and road wear particles, trwp, in the aquatic environment," TRMA, Brussels, Tech. Rep., 2019.
32. Buehler, R., and Pulcher, J., "COVID-19 Impacts on Cycling, 2019–2020", *Transport Reviews*, Vol. 41, No. 4, 2021.
33. Combs, T., and Pardo, C., "Shifting streets COVID-19 mobility data: Findings from a global dataset and a research agenda for transport planning and policy", *Transportation Research Interdisciplinary Perspectives*, Vol. 9, 2021.
34. Dijkstra, E., "A note on two problems in connexion with graph", *Numer. Math.*, Vol. 1, pp. 269-271, 1959.
35. Donati, L., Fontanini, T., Tagliaferri, T. and Prati, R., "An Energy Saving Road Sweeper Using Deep Vision for Garbage Detection", *Applied Sciences*, Vol. 10, No. 22, 2020.
36. Polukarova, M., Markiewicz, A., Björklund, K., Strömwall, A., Galfi, H., Andersson Skölda, Y., Gustafsson, M., Järllskog, I., and Aronsson, M., "Organic pollutants, nano- and microparticles in street sweeping road dust and washwater", *Environment International*, Vol. 135, 2020.

37. Korytov, M., Shcherbakov, V., Titenko, V., Ignatov, S., and Tsekhosh, S., “Mathematical model of the working process of the road sweeping machine as a complex dynamic system”, *Journal of Physics: Conference Series*, Vol. 1441, 2020.
38. Sutton, R., and Barto, A., “Reinforcement Learning: An Introduction”, A Bradford Book, Cambridge, MA, USA, 2018.
39. Sedgewick, R., Wayne, K., “Algorithms”, 4th Edition.. Addison-Wesley, 2011.
40. Overko, R., Ordonez-Hurtado, R., Zhuk, S., Ferraro, P., Cullen, A., and Shorten, R., “Spatial Positioning Token (SPToken) for Smart Mobility”, *IEEE Transactions on Intelligent Transportation Systems*, pp., Accepted and in press, 2020.
41. Even-Dar, E.; and Mansour, Y. 2003. “Learning rates for Q-learning.” *Journal of machine learning*, *Journal of Machine Learning Research*, Vol. 5., pp. 1-25, 2003.